UNIVERSITY OF
BATH

**University of Bath**

# A Summary of Current and New Methods in Velocity Selective Recording (VSR) of Electroneurogram (ENG)

John Taylor, Benjamin Metcalfe & Chris Clarke
Department of Electronics and Electrical Engineering
University of Bath
Bath, BA2 7AY, UK
E-mail: j.t.taylor@bath.ac.uk

Thomas Nielsen
Department of Health Science and Technology
Aalborg University
Aalborg, Denmark

Daniel Chew
Cambridge Centre for Brain Repair
University of Cambridge
Cambridge, CB2 0PY, UK

Nick Donaldson
Department of Medical Physics and Bioengineering
University College London
London, WC1, UK

*Abstract* — **This paper describes the theory of** *velocity selective recording* **(VSR) of neural signals including some new developments. In particular new limits on available selectivity using bandpass filters are introduced and discussed. Existing work has focussed primarily on electrically evoked** *compound action potentials* **(CAPs) where only a single evoked response per velocity is recorded. This paper extends the theory of VSR to naturally occurring neural signals recorded from** *rat* **and describes a practical method to estimate the level of activity (firing rates) within particular velocity ranges.**

*Keywords – Electroneurogram; Velocity Selective Recording; Multielectrode Cuff*

## I. Introduction

*Velocity selective recording* (VSR) is a technique that allows discrimination of action potentials (APs) based both on the direction of propagation (*afferent* or *efferent*) and *conduction velocity* (CV), without the need to submit the nerve to invasive and potentially damaging procedures. Since, for myelinated fibres, there is a well-known relationship between CV and axonal diameter (Erlanger and Gasser 1937 [1]), the VSR method can be used to extract activity related to physiological function from the whole neurogram [2]-[5]. While CV can be calculated using only a single pair of electrodes (a dipole) it has been shown that the *velocity selectivity* of a system, i.e. its ability to discriminate between populations with adjacent CVs propagating simultaneously along the same nerve, can be increased by using multiple electrodes. These can be practically implemented using a *multi-electrode cuff* (MEC), which is now available as a component for use in implantable neuroprostheses. The method provides a viable interface for neural recording systems that have potential use in a range of prosthetic devices, for example the *'Bioelectronic Medicines'* currently being advocated by GlaxoSmithKline [6]. In addition, information about conduction velocity may be useful for neuroscientists wishing to study nerve conduction disorders within the peripheral nervous system.

To date, recordings from cuff-based systems have been made on the assumption that individual APs (spikes) are generally not visible in the time records of individual channels due to poor signal-to-noise ratio. To counter this problem a technique based on bandpass filters was introduced that enables the velocity spectrum of the data to be calculated. This method works well for *compound action potentials* (CAPs), typically evoked by electrical stimulation, but cannot be easily extended to the case of naturally-occurring ENG mostly due to the very small amplitudes of the APs, at least when recorded using nerve cuffs [2]. In addition, in natural ENG, information is encoded as neural firing rates and so it is necessary to determine these rates in a particular velocity band, rather than just the relative amplitudes of activity between bands, which is generally the case for CAPs. These are very demanding requirements on the recording system. However, some recent experimental data obtained from the *vagus* nerve of a *pig* has indicated that, contrary to previous assumptions, simple linear processing of the outputs of an MEC does in fact reveal spike-like patterns of signals in the time record. This observation suggests the possibility of new methods to determine both the activated velocity bands and the level of activity within those bands.

In this paper we begin by surveying existing VSR techniques and propose some fundamental limits on available performance that extends current theoretical knowledge. We then discuss the extension of VSR to the recording of natural ENG and describe our new method of *velocity spectral density* (VSD). This is validated using both simulated data and some preliminary experimental results in *rat*.

## II. Theory and Fundamental Limits of VSR

### A. Basic Principles

The basic principle of VSR is to transform time domain recordings of neural signals into the *velocity domain*. The velocity spectrum, which is computed from the time record of the neural data, shows both the direction of AP propagation (either *efferent* or *afferent*) as well as the level of excitation of each fibre population within the nerve. A simple process termed *delay-and-add* is commonly used to carry out this

transformation [2]. Recordings are made at equal distances along the nerve using a MEC or other linear electrode array such as a microchannel. Each channel is delayed relative to the first channel by an interval that depends on both the electrode spacing and the propagation velocity of the signal. So if the delay between the first two channels is $dt$ the delay between the first and third channels is $2 \cdot dt$ and so on. Delay-and-add operates by inserting variable delays $\tau$ (where $\tau$ is an integer multiple of $dt$) into the channels to effectively cancel the naturally occurring delays after which the channels are summed resulting in a single signal. As the delay is swept through a range values the output goes through a peak when $\tau = d/v$ where $d$ is the inter-electrode spacing and $v$ is the CV of the AP, called the *matched velocity*. So when matching occurs, a pulse (such as an AP) of a particular duration and amplitude on one channel becomes a pulse of the same width and $N$-times the amplitude when the outputs of $N$ channels are summed.

The velocity selectivity of the system is therefore increased by a factor $N$ and the signal to noise ratio by $\sqrt{N}$, assuming the noise sources in each channel are uncorrelated [3]. This leads naturally to the concept of the *velocity quality factor $Q_v$* described in the next section. The resulting velocity profile is called the *intrinsic velocity spectrum* (IVS).

Figure 1 shows the schematic of a typical interface between an MEC and the delay-and-add signal processing. The electrodes are grouped in two ranks: initially in *dipole* pairs ('single differential') and these in turn are connected as *tripoles* ('double differential') although only the dipole circuits are shown in the figure since that was the system used in the experiments described in Section III. These differential arrangements are used to suppress common mode interference signals, most notably the *electromyogram* (EMG). For analysis purposes the MEC is considered to be a linear time invariant (LTI) system with transfer function $H(f, v)$ transforming neural signals (input) into electrical ones (output). The input to the MEC is a *trans-membrane action potential* function (TMAP), $V_m(t)$, with the corresponding spectrum $V_m(f)$. The resulting *single fibre action potential*
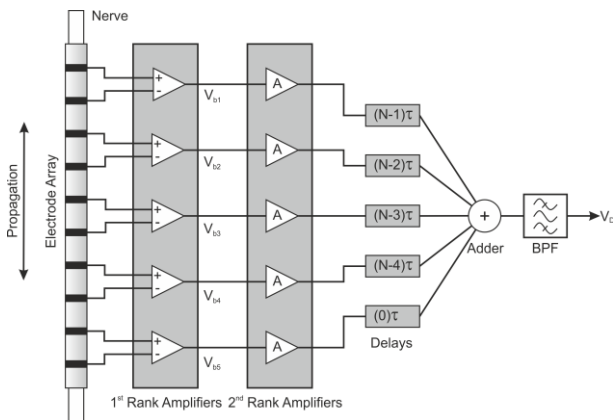


Figure 1: Simplified schematic of the amplifier configuration used to capture neural signals from an MEC. In this arrangement $2N$ electrodes results in $N$ dipole signals. $N$ is typically about 5. In an alternative configuration the electrode connections to the first rank amplifiers are interleaved resulting in $2N - 1$ dipoles.

(SFAP) is a propagating wave with the time dependence of the underlying TMAP function, the relationship between the two being explained in [2]. For the purpose of simulation, we represent the TMAP function and its spectrum by the Fourier transform pair [2]:

$$V_m(t) = At^n e^{-Bt}$$

$$V_m(f) = \frac{n! A}{(B + j2\pi f)^{n+1}} \tag{1}$$

where $A$, $B$ and $n$ are constants and $f$ is frequency. The output $Y(f, v)$, which is a function of both frequency and velocity, is given by eqn (2):

$$Y(f,v) = \left| \frac{\sin\left( N\pi f\left(\frac{d}{v} - \tau\right) \right)}{\sin\left( \pi f\left(\frac{d}{v} - \tau\right) \right)} \right| \cdot 4\frac{R_e}{R_a} \sin^2\left(\frac{\pi f d}{v}\right) \cdot \left| \frac{An!}{(B + j2\pi f)^{n+1}} \right| \tag{2}$$

This equation describes the output of a cuff with $N$ tripoles, electrode spacing $d$ and propagation velocity $v$. $R_a$, the intra-axonal resistance per unit length, has been assumed to be large compared to $R_e$, the extra-axonal resistances per unit length inside the cuff. Equation 2 is the product of the spectrum of the TMAP ($V_m(f)$), the transfer function of one tripole ($H_o(f,v)$), and the transfer function of the delay-and-add block ($G(f,v)$). At *matched velocities* (i.e. where $\tau = d/v$ and $v = v_o$ in eqn (2)), eqn (2) reduces to:

$$Y(f,v_0) = 4N\frac{R_e}{R_a} \sin^2\left(\frac{\pi f d}{v_0}\right) \cdot \left| \frac{An!}{(B + j2\pi f)^{n+1}} \right| \tag{3}$$

The placement of a *bandpass filter* (BPF) in each channel fixes $f$ to the centre frequency of the BPF reducing $Y$ to a function of velocity *only* (this issue was also examined in [7]). Finally, in order to quantify the velocity selectivity, we define a *velocity quality factor*, $Q_v$, by analogy with linear systems in the frequency domain:

$$Q_v = \frac{v_0}{v_{3+} - v_{3-}} \cong \frac{N\pi d}{2.64}\left(\frac{f_0}{v_0}\right) \tag{4}$$

where $v_0$ is the matched velocity and $v_{3+}$ and $v_{3-}$ are the upper and lower 3 dB points respectively. Note that although the proposed arrangement requires a BPF at the output of each channel, in practice, due to the linearity of the processes involved, the summation and filtering operations can be reversed. This leads to a much simpler and more practical arrangement where only a single BPF is required for each velocity band of interest (Fig 1).

### B. Limits on available velocity selectivity; selectivity bandwidth

In order to determine upper and lower bounds on the velocity selectivity generated by an MEC-based recording system, we make the fundamental assumption that BPFs are always used and hence eqn (2) reduces to $Y(v)$, $f$ appearing as a constant ($f_0$).
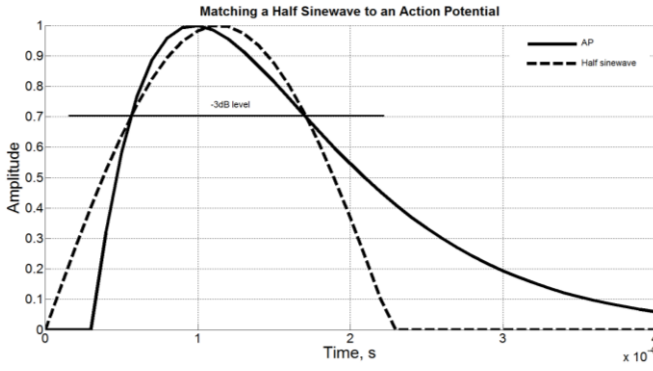
Figure 2. Fitting half a sinewave (dashed line) to an AP (solid line) to find the lower bound on velocity selectivity. The matching is in the time domain at the -3 dB points of the curves.

Using eqn (4) calculation of the range of available velocity selectivity (expressed as $Q_v$) at a velocity $v_0$ reduces to finding the range of possible values of $f_0$, which might appropriately be called the *selectivity bandwidth*.

*(a) Lower bound:* this is taken to be the frequency of a sinewave whose width most nearly matches the positive phase of an AP of the same amplitude, as illustrated in Fig 2. This is an approximation to the *intrinsic velocity selectivity* (IVS). The matching is carried out at the -3 dB points of both waveforms and it can be shown that, to a good level of approximation, the equivalent frequency $f_L$ is given by:

$$f_L \cong \frac{B}{8} \tag{5}$$

Where the parameter $B$ relates to $V_m(t)$ in eqn (1). So, for example, if $B = 15$ kHz, $f_L = 1.875$ kHz (approximated to 2 kHz for simulation) and hence substituting into eqn (4) with $d = 3$ mm and $N = 10$, the lower bound on $Q_v$ at $v_0 = 30$ m/s is 2.2.

*(b) Upper bound:* In [4] we noted that the upper bound on velocity selectivity is set by noise considerations because the spectrum of the signal (see eqn (3)) decreases monotonically with frequency eventually merging with the noise floor of the system. Clearly the signal has no energy left beyond this frequency to drive a BPF and so it seems reasonable to choose this 'noise corner frequency' as the upper frequency limit that also determines the maximum available velocity selectivity. In the example in Fig 3, the spectrum of a single monopolar AP is plotted with and without additive white noise. The form of the AP is given by eqn (1) with $A = 40,774$ V, $B = 15,000$ Hz and $n = 1$. These constants are chosen to be representative of a mammalian AP normalised to peak amplitude of unity. The noise generator employed produces zero mean Gaussian white noise with instantaneous power $\sigma^2$ and so for a sequence length $L$ the mean power is $\sigma^2/L$ and the *rms* power is $\sigma/\sqrt{L}$. For example if $\sigma = 0.1$ and $L = 1024$, the *rms* power is 3.125 x $10^{-3}$ W.

Note that the spectrum of the noise is actually flat and the oscillations shown are an artefact of the FFT process for a finite length sequence.
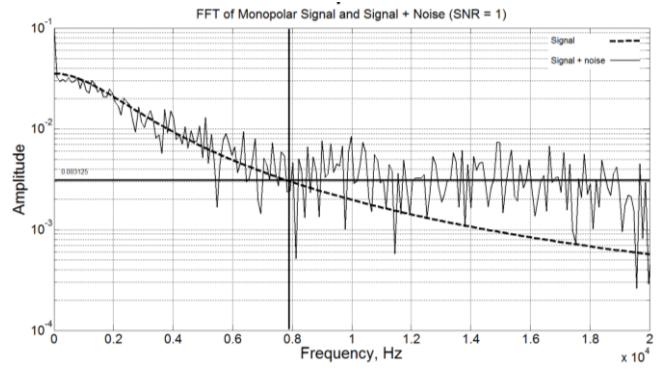


Figure 3. Spectrum (1024 point FFT) of a single monopolar AP (dashed curve) and the same with additive white Gaussian noise (solid curve). In this example $\sigma = 0.1$ (SNR $\approx 1$) and so the noise floor is 3.125 x $10^{-3}$ V. The spectra intersect at a frequency of approximately 7.7 kHz. This 'noise corner' frequency is taken to be the maximum frequency at which a BPF can operate and therefore defines the maximum available velocity selectivity.

The spectrum of the TMAP function is described by the continuous time Fourier Transform (CTFT) in eqn (3) but it should be noted that the spectrum shown in Fig 3 was calculated using a 1024 point FFT with a sampling frequency of 100 kHz. The two representations are very similar for frequencies well below the Nyquist limit (50 kHz in this case) but closer to this limit the two plots diverge somewhat. However, the single sided CTFT produces a particularly simple analytical expression for the signal and was adopted in this paper:

$$V_m(\omega) = \frac{2F_s}{L} \frac{A}{(B + j\omega)^2}$$

and so:

$$|V_m(\omega)| = \frac{2F_s}{L} \frac{A}{B^2 + \omega^2} \tag{6}$$

In order to calculate the noise corner frequency $\omega_{lim}$ it is necessary to set $|V_m(\omega)|$ equal to $\sigma/\sqrt{L}$ and solve for $\omega_{lim}$:

$$\omega_{lim} = 2\pi f_{lim} = B\sqrt{\frac{2AF_s}{\sigma\sqrt{L}B^2} - 1}$$

we can write the complete expression for the *selectivity bandwidth*:

$$\frac{B}{8} \leq f_0 \leq \frac{B}{2\pi}\sqrt{\frac{2AF_s}{\sigma\sqrt{L}B^2} - 1} \tag{7}$$

It is useful to express this in terms of the *signal to noise ratio* (SNR). The average (*rms*) signal power is calculated from the TMAP function as follows:

$$P_s = A\sqrt{\frac{1}{\tau}\int_0^\tau t^2 e^{-2Bt} dt} \cong \frac{A}{2\sqrt{\tau}B^{3/2}}$$

where $\tau$, the length of the sequence is $LT_s = L/F_s$. Combining this with the expression for the *rms* noise:

$$SNR = \frac{A\sqrt{F_s}}{2\sigma\sqrt{L}B^{3/2}} \tag{8}$$

Using this expression, eqn (7) can be rewritten in a more compact form:

$$\frac{B}{8} \leq f_0 \leq \frac{B}{2\pi}\sqrt{4\left(\frac{F_s}{B}\right)^{0.5}(SNR)-1}$$

and, finally, recalling that SNR increases as a function of $\sqrt{N}$, we can write:

$$\frac{B}{8} \leq f_0 \leq \frac{B}{2\pi}\sqrt{4\left(\frac{NF_s}{B}\right)^{0.5}(SNR)-1} \quad (9)$$

Since the ratio of velocity selectivity enhancement, $R_s$, is proportional to this *selectivity bandwidth* (see eqn (4)), we can write:

$$R_s \cong \frac{8}{\pi}\left(\frac{NF_s}{B}\right)^{0.25}(SNR)^{0.5} \quad (10)$$

So, e.g., with the parameter values given above and $SNR = 1$, $R_s = 11.7$, a significant level of velocity selectivity enhancement. Note that $R_s$ changes very slowly as the parameters $N$, $F_s$ and $B$ are varied but more rapidly with $SNR$.

### C. Simulation results

The 10-channel system discussed above was simulated using MATLAB for the three values of SNR tabulated plus the noiseless case (i.e. SNR → ∞). The resulting selectivity parameters are given in Table I. Fig 4 shows the IVS for a single AP propagating at 30 m/s for these four values of SNR. For the case where $SNR = 10$ the profile is indistinguishable from the noiseless case. For $SNR = 1$ there is some degradation of performance but for $SNR = 0.1$ the method fails completely. This is entirely consistent with the values given in Table I since the delay-and-add process fails when $f_{lim}$ falls below the lower limit given by (5).

Table I
Relationship between SNR and the Selectivity Bandwidth

| calculated from eqn (8) | | $f_{lim}$ (kHz) calculated from eqn (9) | | Selectivity BW (kHz) | |
|---|---|---|---|---|---|
| σ | SNR | N = 1 | N = 10 | N = 1 | N = 10 |
| 0.01 | 11 | 25.3 | 45.16 | 23.3 | 43.16 |
| 0.1 | 1.1 | 7.7 | 14.12 | 5.7 | 12.12 |
| 1.0 | 0.11 | 0.88 | 3.85 | - | 1.85 |

### D. Experimental results

Some preliminary experiments were carried out to assess the applicability of VSR to recording naturally evoked (physiological) ENG using an MEC. The right *vagus* nerve of a Danish Landrace *pig* was fitted with an MEC of length 4 cm containing ten annular electrodes with a pitch of 3.5 mm. Bipolar measurements of ENG were made with the animal at rest. A short segment of each of the resulting nine channels of data (original duration 2 minutes and sampled at 100 kS/s with 16-bits resolution) is shown in Fig 5.
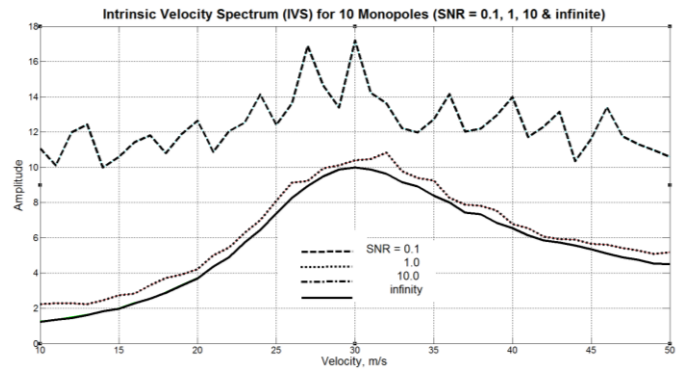


Figure 4. IVS for a 10 channel system with added white noise. Three values of *SNR* are indicated (10, 1 and 0.1) in addition to the noiseless case. Note that for *SNR* = 10 the profile is indistinguishable from the noiseless case. For *SNR* = 1 there is some degradation of performance but for *SNR* = 0.1 the method fails completely.

Examination of the traces in Fig 5 shows no discernable features that could be attributable to ENG activity. However when delay-and-add is applied, as shown in Fig 6 for matched velocities in the range 31 – 45 m/s with an interval of 2 m/s, correlated peaks are clearly visible revealing several excited populations including the one illustrated in the figure at 37 m/s.

The ability to recover correlated data from nerve cuff recordings using an MEC results directly from the improvement in SNR provided by the delay-and-add process as discussed above. This result is significant as it suggests not only that practical VSR systems can be used to record physiological data using MECs but also suggests a technique to extract information from the nervous system based on axonal firing rates. Such a method is discussed in the next section.

### III. VELOCITY SPECTRAL DENSITY

#### A. Basic method

VSR is well suited to the analysis of single event APs such as those typically found in electrically evoked CAPs. Information within the nervous system is transmitted in an encoded fashion; the number of APs propagating through a single axon per second is representative of the sensory (analogue) input signal to that axon [8]. This feature is a direct result of the *all-or-nothing* nature of the neuron. As an example, the *afferent* fibres that contain information about the fullness of the bladder have been measured in man to propagate at a velocity of 41 m/s with a baseline firing rate of about 15 APs per 200 ms and a rate representing a full bladder of about 40 APs per 200 ms [9]. The contribution of this section of the paper is to propose an extension to VSR to include information about the number of APs occurring in a given time period. The result is called the method of *velocity spectral density* (VSD) and provides a measure of the time varying activity within a band of conduction velocities [10]. One method for extracting both conduction velocity and neuronal firing rates from a nerve recording is to use a sliding time window of sufficient length to enclose only a single AP. Delay-and-add can then be applied to extract the IVS of the
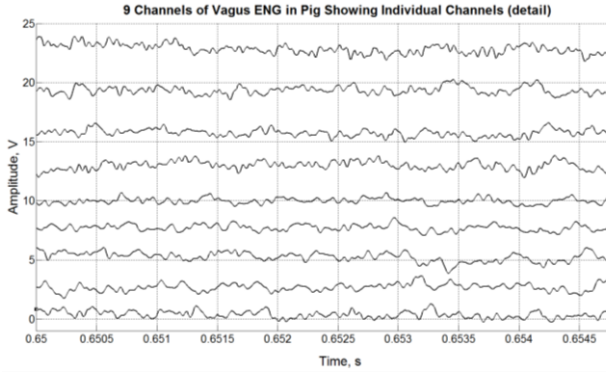
Figure 5. A short segment of nine bipolar channels of recorded ENG from the right *vagus* nerve of a *pig* (the animal was at rest). An MEC of length 4 cm fitted with ten annular electrodes with a pitch of 3.5 mm. Note that there are no discernable features attributable to ENG activity.
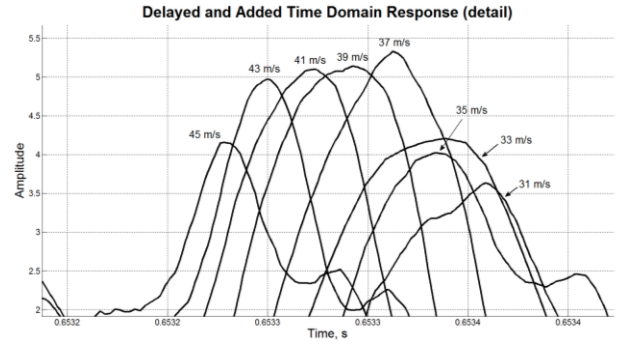


Figure 6. Detail of the data in Fig 5 after delay-and-add has been applied for a range of matched velocities from 31 to 45 m/s in steps of 2 m/s. Note that correlated peaks are clearly visible.

window contents and thus identify the most likely conduction velocity for the AP based on the velocity of the peak value, $V_{peak}$. This process could be repeated as the window is moved along the time record and the firing rates extracted by simply counting the number of occurrences of each velocity but this has two significant drawbacks. Firstly, the window must only contain a single AP, otherwise only the AP with the largest amplitude will be identified as the largest peak in the IVS. Secondly the windowing function must be carefully selected to avoid *velocity spectral leakage* (VSL), an effect that is similar to spectral leakage in the frequency domain, resulting from the time domain window failing to encompass the AP fully. A more robust method has been developed that does not require the use of a sliding time window and so avoids these issues. The new method by which both conduction velocity and neuronal firing rates can be extracted is described in the following steps.

1. A set of time records of arbitrary length is processed using the delay-and-add method as described above. The values of *dt* used can be selected, based on the required velocity range and resolution. For example a velocity range of 10 - 50 m/s with an electrode spacing of 1 mm requires *dt* values in the range 20 - 100µs. If the resolution is 1 m/s then this will result in a set of 41 $V_D$ waveforms, one for each velocity and formed by simple summation of the delayed signals. The form of $V_D$ for each value of *dt* over 5 channels of raw data is given by:

$$V_D(t, dt) = \sum_{i=1}^{5} V_{Bi}(t(i-1) \cdot dt)$$

2. A simple hard noise threshold is applied that removes any samples below the system noise floor. At present the noise floor for experimental results is computed from the input-referred noise as measured during the experiments.

3. In order to identify an AP the relationship between $V_D$ for neighbouring values of *dt* must be examined. Each $V_D$ waveform is passed through a filter that detects the centroid of each AP [10]. This filter is

implemented as a linear finite impulse response (FIR) filter with impulse response h[n] given in eqn (11):

$$h[n] = -(2/N)n + 1 \qquad (11)$$

This is a linear function of gradient -2/N where N is the width of the filter and *n* is the current index of the discrete-time samples. The function *h[n]* varies in amplitude from +1 to -1 where N is chosen to be at least as wide as a single AP in the time domain. Since in practice the APs are neither regular nor symmetric the centroid represents a more robust method for locating the midpoint of the AP than taking the maximum value as has been done previously. The centroid can be considered as the geometric centre of any two dimensional region, in this case the area under the AP as bounded by the *x* axis. It is necessary to separate the positive and negative phases of the AP before locating the centroid, and this was achieved via half wave rectification of the signal. Computing the centroid considers the contribution from every sample as opposed to the single samples used in peak detection and so it is more robust against noise and interference.

4. Finally a detection algorithm is applied that examines each velocity response for the criterion $V_{D-1} < V_D > V_{D+1}$. If this criterion is met the histogram for the current window can be incremented at the velocity $V_D$.

The signal processing requirements for VSD are conceptually minimal. In a practical system designed for implementation within a VLSI architecture the largest components are the delay lines associated with the delay-and-add process and the centroid FIR filter. Generally speaking the band-pass filters are realised using 4th order Butterworth structures for which both area and power efficient versions are readily available. The driving force behind implantable systems is power consumption and the methods described within this paper are well suited to low power VLSI implementations using pre-existing and scalable technologies.

### B. Preliminary measured results

In order to provide some preliminary validation of the VSD process, acute *in-vivo* recordings were made from a *rat* [11]. These experiments were part of a larger study that is not included here. The recording setup consisted of five bipolar recordings taken from a set of six hook electrodes placed on a fascicle of the L5 *dorsal* root. For consistency with the simulated data, the electrode spacing was 1 mm and the sample rate was 500 kS/s. The data were captured and processed using MATLAB in the same manner as the simulated data reported above. The recordings were of length 250 ms and were made both with and without cutaneous stimulation of the L5 dermatome. In order to identify the effect of cutaneous stimulation of the dermatome, direct electrical stimulation was used to identify the conduction velocities of the relevant *afferents*.
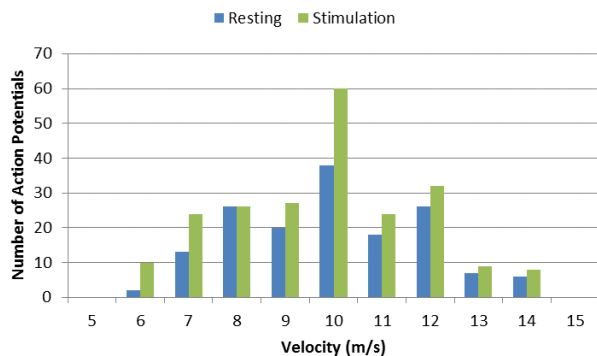


Figure 7. VSD histogram recorded from 250ms of physiological recordings from *rat* during both a resting state and during cutaneous stimulation.

VSD analysis applied to the data showed consistent levels of activity in both sets of natural recordings with a significant increase in the number of APs propagating at 10 m/s during cutaneous stimulation (Fig. 7). This was in agreement with direct electrical stimulation of the dermatome where CAPs were observed with a conduction velocity of 10 m/s. The velocity band 10 m/s – 17 m/s is within the accepted range of conduction velocities for the *Aδ afferent* fibres in rat, which are responsible for light touch sensation.

## IV. CONCLUSION

This paper has reviewed two related topics of current interest in neural recording. Firstly, the method of *velocity selective*

*recording* (VSR) was reviewed and new performance limits were introduced. Secondly, a new method that extends significantly the capabilities of VSR using an automated detection system and a histogram-based analysis of neuron firing rates, was described. The method generates a detailed overview of the firing rates of neurons based on conduction velocity and direction of propagation. This was demonstrated for both simulated data and *in-vivo* physiological recordings from the L5 dorsal root in *rat*.

## VI. REFERENCES

[1] H. Gasser, "The classification of nerve fibers.," *Ohio Journal of Science*, vol. 41, no. 3, pp. 145–159, 1941.

[2] Taylor J., Donaldson N., & Winter J. (2004) "The use of multiple-electrode nerve cuffs for low velocity and velocity-selective neural recording." *Med. & Biol. Eng. & Comput.*, 42 (5), 634-43.

[3] N. Donaldson, R. Rieger, M. Schuettler, and J. Taylor, "Noise and selectivity of velocity-selective multi-electrode nerve cuffs.," *Med. Biol. Eng. Comput.*, vol. 46, no. 10, pp. 1005–18, Oct. 2008.

[4] J. Taylor, M. Schuettler, C. Clarke, and N. Donaldson, "The theory of velocity selective neural recording: a study based on simulation.," *Med. Biol. Eng. Comput.*, vol. 50, no. 3, pp. 309–18, Mar. 2012.

[5] Yoshida, K., Kurstjens, G., & Hennings, K. (2009) "Experimental validation of the nerve conduction velocity selective recording technique using a multi-contact cuff electrode." *Medical Engineering & Physics* 31 1261-1270.

[6] K. Famm, B. Litt, K. J. Tracey, E. S. Boyden, and M. Slaoui, "Drug discovery: a jump-start for electroceuticals.," *Nature*, vol. 496, no. 7444, pp. 159–61, Apr. 2013.

[7] Karimi, F, Seydnejad, S, "Velocity selective neural signal recording using a space-time electrode array", *IEEE Transactions on Neural Systems and Rehabilitation Engineering,* issue 99, 2014.

[8] H. Milner-Brown, R. Stein, and R. Yemm, "Changes in firing rate of human motor units during linearly changing voluntary contractions," *The Journal of physiology*, pp. 371–390, 1973.

[9] G. Schalow, G. Zäch, and R. Warzok, "Classification of human peripheral nerve fibre groups by conduction velocity and nerve fibre diameter is preserved following spinal cord lesion," *Journal of the autonomic nervous system*, vol. 1838, no. 6, 1995.

[10] B. Metcalfe, D. Chew, C. Clarke, N. Donaldson, and J. Taylor, "An enhancement to velocity selective discrimination of neural recordings: Extraction of neuronal firing rates.," *Annu. Int. Conf. IEEE Eng. Med. Biol. Soc.*, vol. 2014, pp. 4111–4, Aug. 2014.

[11] B. Metcalfe, D. Chew, C. Clarke, N. Donaldson, and J. Taylor, "Fibre-selective discrimination of physiological ENG using velocity selective recording: Report on pilot rat experiments," *Annu. Int. Conf. IEEE Eng. Med. Biol. Soc.*, vol. 2014, pp. 2645–8, Aug. 2014.